Lattice-Geometry Effects in Garnet Solid Electrolytes: A Lattice-Gas Monte Carlo Simulation Study

Benjamin J. Morgan[1]

[1] *Department of Chemistry, University of Bath, Claverton Down, Bath, BA2 7AY*

(Dated: June 30, 2017)

In many solid electrolytes, ion transport can be approximated as a sequence of hops between distinct lattice sites. Assuming these hops are uncorrelated allows quantitative relationships to be derived between microscopic hopping rates and macroscopic transport coefficients; tracer diffusion coefficients and ionic conductivities. In real materials, hops are uncorrelated only in the dilute limit, where interactions between mobile ions can be neglected. At non-dilute concentrations these interactions can be significant, causing hops to become correlated. In these cases the relationships between hopping frequency, diffusion coefficent, and ionic conductivity deviate from the random walk expressions, with this deviation quantified by single-particle and collective correlation factors, f and f_{I}. These factors vary between materials, and depend on the concentration of mobile particles, the nature of the interactions, and the host lattice geometry. Here we study these correlation effects for the garnet lattice using lattice-gas Monte Carlo simulations. This lattice represents diffusion pathways in lithium-garnets—a family of promising solid lithium-ion electrolytes—and has an unusual geometry containing both 4-coordinate and 2-coordinate sites. We find that for non-interacting particles (volume exclusion only) single-particle correlation effects are more significant than for any other known three-dimensional solid-electrolyte lattice. This is attributed to the presence of 2-coordinate lattice sites, which causes correlation effects intermediate between typical three-dimensional and one-dimensional lattices. By including nearest-neighbour repulsion and on-site energies we predict more complex single-particle correlations and also collective correlations. We predict particlularly strong correlation effects at $x(\mathrm{Li}) = 3$ (from site energies) and $x(\mathrm{Li}) = 6$ (from nearest-neighbour repulsion). Both effects correspond to ordering of the mobile particles over the lattice. Finally we consider the question of how mobile ion stoichiometry can be tuned to maximise the ionic conductivity, and show that the "optimal" lithium content is highly sensitive to the precise nature and strength of the microscopic interactions.

I. INTRODUCTION

The ability of solid electrolytes to conduct electric charge by transporting ions is central to their use in devices such as fuel cells and solid-state lithium-ion batteries.[1–4] In both cases, solid electrolytes with high ionic conductivities are desirable. In fuel cells high conductivities allow lower operating temperatures, reducing running costs and increasing operating lifetimes. In solid-state batteries high conductivities allow faster charging rates and higher power outputs. Ionic conductivities depend on a number of factors, including the crystal structure, the chemical composition, and the concentration of mobile ions.[5] Developing a quantitative understanding of these factors is key to developing high conductivity solid electrolytes for use in high performance electrochemical devices.

Solid electrolytes can be considered to comprise two distinct sets of ions: "fixed" ions that vibrate about their crystallographic sites, and "mobile" ions that diffuse through the system and contribute to ionic conductivity. The fixed ion positions define a network of diffusion pathways through which the mobile ions move. Solid electrolytes with common crystal structures have diffusion networks that are topologically equivalent, while electrolytes with different crystal structures will have topologically distinct diffusion paths. While much research into solid electrolytes focusses on understanding differences in ionic conductivities within specific structural families, a complementary question considers how differences in crystal structure, and hence diffusion network topology, affect ionic transport.

Crystal structure can be considered a microscopic characteristic, dictating the positions of individual atoms. Ionic transport at scales relevant to device performance, however, is described by macroscopic transport coefficients: diffusion coefficients and ionic conductivities. These describe long-time behaviours, and represent ensemble averages over all microscopic diffusion processes. A meaningful understanding of differences in ionic conductivity between solid electrolytes therefore depends on the quantitative relationships between microscopic diffusion and macroscopic ion transport. This study considers these relationships for the lithium-garnet family of solid lithium-ion electrolytes, using lattice-gas Monte Carlo simulations.

In many solid electrolytes, the microscopic transport of ions can be approximated as a sequence of discrete "hops" between distinct lattice sites.[6] If these hops are *independent*, every ion follows a random walk. The tracer diffusion coefficient, D^*, and ionic conductivity, σ, can then be expressed in terms of the average hop-rate per atom, $\widetilde{\nu}$,[7] via[8,9]

$$D^* = \frac{1}{6} a^2 \widetilde{\nu}; \tag{1}$$

$$\sigma = \frac{Cq^2}{kT}\frac{1}{6}a^2\widetilde{\nu}; \tag{2}$$

where a is the characteristic hop distance, C is the mobile ion concentration, and q is the charge of the mobile ions. Equations 1 and 2 can be combined to give the Nernst-Einstein relation, which connects D^* and σ:

$$\frac{\sigma}{D^*} = \frac{Cq^2}{kT}. \tag{3}$$

These three equations provide quantitative relationships between the hop-rate, $\widetilde{\nu}$, tracer diffusion coefficient, D^*, and ionic conductivity, σ. Their derivation, however, depends on the assumption of independent hops, which holds only in the limit of very low carrier concentrations, or for fully non-interacting mobile ions.[10]

Practical solid electrolytes typically have high carrier concentrations, and interparticle interactions can be significant. In these cases, hopping probabilities depend on specific arrangements of nearby ions, and hops are no longer statistically independent. Instead, ion trajectories are *correlated*, and the system dynamics deviates from random walk behaviour.[8,11–13] Correlations between hops made by any single ion modify the relationship between average hop rate, $\widetilde{\nu}$, and tracer diffusion coefficient, D^*, which becomes

$$D^* = \frac{1}{6}a^2\widetilde{\nu}f, \tag{4}$$

where f is a single-particle correlation factor that accounts for the deviations from random walk behaviour. Correlations between hops made by *different* ions modify the relationship between $\widetilde{\nu}$ and σ, which becomes

$$\sigma = \frac{Cq^2}{kT}\frac{1}{6}a^2\widetilde{\nu}f_{\mathrm{I}}, \tag{5}$$

where f_{I} is a collective or "physical" correlation factor.[10,14,15] The relationship between σ and D^* now differs from Nernst-Einstein behaviour (Eqn. 3) by the ratio of these correlation factors:

$$\frac{\sigma}{D^*} = \frac{Cq^2}{kT}\frac{f_{\mathrm{I}}}{f}. \tag{6}$$

The inverse ratio $\frac{f}{f_{\mathrm{I}}}$ is commonly denoted as the Haven ratio, H_{R}[10,16].

Quantitative relationships between microscopic hopping rates and macroscopic transport coefficients can, in principle, be obtained by combining experimental data for $\widetilde{\nu}$, D^*, and σ. Ion hopping rates may be measured from NMR or muon spin-relaxation experiments,[17–22] diffusion coefficients obtained from tracer diffusion experiments,[23] and ionic conductivities derived via impedence spectroscopy.[24,25] Computational methods provide an increasingly useful complement to experimental studies. First principles calculations of vibrational partition functions and barrier heights along diffusion pathways can be used to obtain hopping rates.[26,27] Molecular dynamics simulations can be used to directly calculate diffusion coefficients and ionic conductitivies.[28] Often, however, not all members of $\{\widetilde{\nu}, D^*, \sigma\}$ are known, and it is necessary to derive one or more from the other, known, properties. In principle, quantative conversions between $\{\widetilde{\nu}, D^*, \sigma\}$ are possible via Eqns. 4–6, providing the correlation factors f, f_{I} (and hence H_{R}) are known.

For many simple crystal lattices, the correlation parameters $\{f, f_{\mathrm{I}}, H_{\mathrm{R}}\}$ have been calculated.[10,29] For more complex crystal structures, however, these parameters are often still unknown. A common approximation, therefore, is to assume correlation effects can be neglected, which allows the simpler Eqns. 1–3 to be used. This approximation is equivalent to assuming dilute-limit non-interacting behaviour. In solid electrolytes ionic motion exhibits strong correlations, however, this can introduce quantitative errors when analysing data.

In this study, we describe lattice-gas Monte Carlo simulation of garnet-structured solid electrolytes, to study quantitative correlation effects in these materials. The garnet lattice represents the diffusion pathways in the "lithium-garnets". This family of solid lithium-ion electrolytes $\mathrm{Li_xM_3M'_2O_{12}}$,[30,31] have attracted significant attention as candidates for all–solid-state lithium-ion batteries.[1,32–34] The garnet crystal structure has an unusual three-dimensional network of lithium diffusion pathways, consisting of interlocking rings.[35] Each ring comprises 12 alternating tetrahedral and octahedral sites. The tetrahedral sites are are coordinated to four octahedral sites, while the octahedral sites are each coordinated to two tetrahedral sites. The tetrahedral sites therefore act as nodal points connecting adjacent rings (Fig. 1). Aliovalent substitution of the M and M' cations allows the lithium stoichiometry to be tuned across a broad range. A lithium stoichiometry of $x_{\mathrm{Li}} = 9$ corresponds to a fully occupied lithium-site lattice, and research has focussed on "lithium stuffed" garnets, typically with $x_{\mathrm{Li}} = 5$ to 7. Ionic conductivities vary enormously as a function of x_{Li}, with σ increasing by $\sim 10^9$ between $\mathrm{Li_3Tb_3Te_2O_{12}}$ and $\mathrm{Li_{6.55}La_3Zr_2Ga_{0.15}O_{12}}$,[1,31] and it remains an open question precisely how the lithium diffusion coefficient and ionic conductivity vary with lithium stoichiometry. It is also not know to what extent the unusual diffusion pathway topology affects ionic transport. Resolving these questions is critical for the optimisation of ionic conductivity for this family of materials.

Structural considerations and published data both suggest lithium-garnets may exhibit significant correlation effects. The low connectivity of the two-coordinate octahedral sites means blocking effects are expected to be considerable.[35] Short distances between neighbouring lattice sites of $\sim$ 2.4 Å suggest strong Li–Li repulsion, with particular significance at high Li stoichiometries.[36–39] The presence of two non-equivalent sets of lattice sites is also a factor. Non-interacting lithium ions would be expected to occupy octahedral and tetrahedral sites in a 2:1 ratio, reflecting the rela-

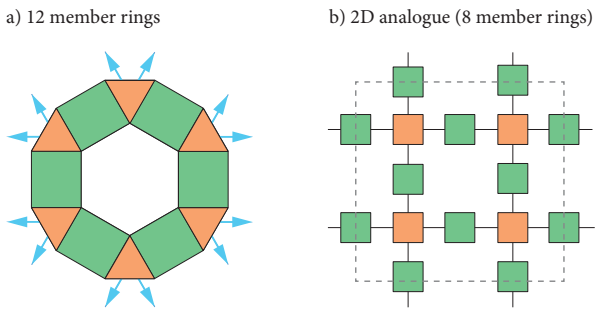

FIG. 1. Schematic of the ring structures that constitute the garnet lithium-diffusion network. a) Each ring consists of 12 alternating tetrahedra (orange) and octahedra (blue). Arrows show connections to neighbouring rings.[35] b) A 2D analogue of interconnected 8-membered rings of alternating "tetrahedra" and "octahedra".

tive site populations. Neutron data, however, show that at low lithium content ($x_{\mathrm{Li}} = 3$) only tetrahedral sites are occupied,[40] while at higher lithium content ($x_{\mathrm{Li}} = 5 \rightarrow 7$) octahedral sites become preferentially occupied.[31,38] Experimental conductivities show non-linear dependence on x_{Li},[41] and deviate strongly from ideal values predicted (via Eqn. 2) from muon-spin–spectroscopy hopping rates.[21] Further evidence for correlated transport in lithium garnets comes from computational studies. A variety of correlated diffusion processes have been observed in molecular dynamics simulations,[42–45] and calculated diffusion coefficients and ionic conductivities show non–Nernst-Einstein behaviour ($H_{\mathrm{R}} < 1$).[46,47] Together, these results indicate the existence of significant interactions, either between lithium ions or between these ions and the host lattice. The quantitative effects of correlation in lithium garnets, however, are not known, and consequently studies often rely on assumptions of uncorrelated motion to convert between hop rates, diffusion coefficients, and ionic conductivities.[21,22,24,42,48–56]

Here we present a computational study of these correlation effects, comprising lattice-gas kinetic Monte Carlo simulations of diffusion on a garnet lattice, across a range of model Hamiltonians. We calculate f and f_{I} as functions of lithium stoichiometry (carrier concentration), first for a non-interacting volume-exclusion model,[57] and then for models that include on-site single-particle energies and/or nearest-neighbour repulsion interactions. In addition to self- and collective-correlation factors, we present site occupation populations, diffusion coefficients, and reduced ionic conductivities for this range of simulation models. Our results demonstrate how different interactions contribute to non-ideal behaviour, and modify the relationships between particle hopping rate, diffusion coefficient, and ionic conductivity.

We find that for non-interacting particles (volume exclusion only) single-particle correlation effects are more significant than for any other 3D solid electrolyte lattice. This is attributed to the presence of 2-coordinate lattice sites, which produces correlation effects intermediate between typical 3D and 1D lattices. Including nearest-neighbour repulsion and on-site energy differences gives more complex single-particle correlation behaviour and introduces collective correlation. In particular, we find strong correlation effects at $x_{\mathrm{Li}} = 3$ (due to site energy differences) and $x_{\mathrm{Li}} = 6$ (due to nearest-neighbour repulsion). Both effects correspond to ordering of the mobile particles over the lattice, and sharp decreases in diffusion coefficients and ionic conductivities. Finally we consider the question of how mobile ion stoichiometry can be tuned to maximise the ionic conductivity. We find this does not have a straightforward answer, and the optimal stoichiometry is highly sensitive to the choice of interaction parameters.

II. METHODS

Lattice-gas Monte Carlo simulations describe the diffusion of a set of mobile ions populating a host lattice, expressed as a graph of interconnected sites.[58] Every lattice site is either occupied or vacant, and during a simulation the mobile ions undergo a sequence of hops from site to site. These hops are randomly selected, with relative probabilities that satisfy the principle of detailed balance and represent the underlying model Hamiltonian. The simplest model considered here is a non-interacting volume-exclusion–only model.[59] Double occupancy of sites is forbidden, and allowed hops are all equally likely. Non-interacting models allow the pure geometric effect of the lattice to be evaluated, but neglect other interactions that may be important in otherwise equivalent experimental systems. Here we extend the non-interacting model to also consider the effect of nearest-neighbour interactions between mobile ions, described by a nearest-neighbour repulsion energy, E_{nn}, and interactions between single ions and the lattice, described by on-site energies for tetrahedral versus octahedral sites, E_{tet}, E_{oct}. The energy of any configuration of occupied sites, j is given by

$$E = \sum_j n_j^{\mathrm{nn}} E_{\mathrm{nn}} + E_{\mathrm{site}}^j, \tag{7}$$

where n_j^{nn} is the number of occupied nearest neighbour sites for (occupied) site j. For interacting systems, the relative probability of hop i depends on the change in total energy if this hop was selected, ΔE_i,

$$P_i \propto \begin{cases} \exp\left(\frac{\Delta E_i}{kT}\right), & \text{if } \Delta E_i > 0 \\ 1, & \text{otherwise.} \end{cases} \tag{8}$$

For our interacting systems, the change in energy for each candidate hop can depend on the change in number of nearest-neighbour interactions and the change in on-site energy for moving from a tetrahedral to octahedral site (or vice versa):

$$\Delta E_i = \Delta n_{\mathrm{nn}} E_{\mathrm{nn}} \pm \Delta E_{\mathrm{site}}, \tag{9}$$

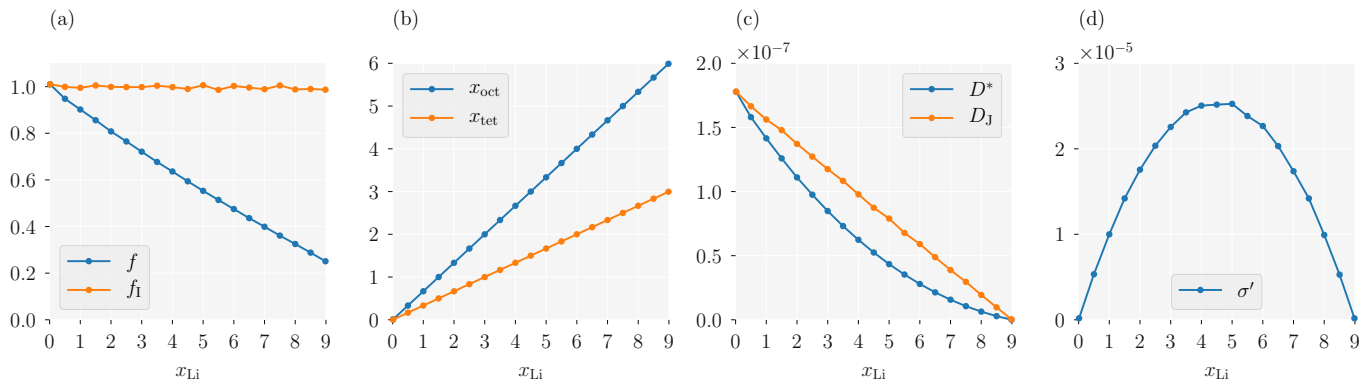

FIG. 2. Non-interacting particles on a garnet lattice: (a) The single-particle correlation factor, f, and collective correlation factor, f_I; (b) Average octahedral and tetrahedral site occupations per forumla unit, x_{oct} and x_{tet} c) Tracer diffusion coefficient, D^*, and "jump" diffusion coefficient D_J. d) Reduced ionic conductivity, σ'.

where $\Delta E_{site} = E_{oct} - E_{tet}$. At each simulation step, one hop is randomly selected according to the set of relative probabilities. The corresponding ion is moved, and a new set of relative hop probabilities is generated for the subsequent simulation step.

In the limit of a large number of hops, the tracer- and collective-correlation factors can be evaluated as

$$f = \frac{\sum_i \langle R^2 \rangle}{Na^2}, \tag{10}$$

where $\langle R^2 \rangle$ is the mean-squared displacement of the mobile ions, and N is the total number of hops during the simulation,[26] and

$$f_I = \frac{|\sum_i R_i|^2}{Na^2}, \tag{11}$$

where $\sum_i R_i$ is the *net* displacement of all mobile particles. In both cases the denominators correspond to the limiting behaviour for uncorrelated diffusion.

To allow time-dependent properties to be evaluated, such as average site occupations and transport coefficients, we perform our simulations within a rejection-free kinetic Monte Carlo scheme.[60] At each simulation step, k, the set of relative hop probabilities, $\{P_{i,k}\}$, are converted to rates, $\{\Gamma_{i,k}\}$, by scaling by a common prefactor $\nu' = 10^{13}\,\mathrm{s}^{-1}$. After selecting a hop, the simulation time is updated by $\Delta t = Q_k^{-1} \ln(1/u)$, where Q_k is the "total rate"; $Q_k = \sum_i \Gamma_{i,k}$, and u is a uniform random number $u \in (0, 1]$.

Our lattice-gas kinetic Monte Carlo simulations were performed using the `lattice_mc` code.[61] Simulations were performed for an ideal cubic $2 \times 2 \times 2$ garnet lattice, with 384 octahedral sites and 192 tetrahedral sites. The lattice-site coordinates were generated from the cubic high-temperature $Li_7La_3Zr_2O_{12}$ (LLZO) structure,[35] using the centres of the octahedra and tetrahedra defined by the oxide sublattice. In cubic LLZO, each lithium-octahedron contains a "split" pair of distorted 96h sites, separated by 0.81 Å. The construction used here considers each octahedron as a single ideal 48g site. The graph of diffusion pathways includes connections between nearest-neighbour sites only, i.e. all connections are between neighbouring tetrahedral–octahedral pairs. For each simulation, n_{Li} mobile ions are randomly distributed across the lattice sites. We perform 1,000 steps for equilibration, followed by 10,000 production steps.

For each set of model parameters, $\{E_{nn}, \Delta E_{site}\}$, simulations were performed across the full range of possible lithium stoichiometry. For a $2 \times 2 \times 2$ garnet supercell, the maximum Li content of $x_{Li} = 9$ corresponds to $n_{Li} = 576$. For each set of interaction parameters, data were collected as an average over 5,000 independent trajectories.

III. RESULTS

A. Non-Interacting Particles and Geometric Effects

We first examine the pure geometric effect of the garnet lattice by considering non-interacting particles, where any deviations from random walk behaviour are solely due to blocking effects expressed within the specific lattice geometry. Fig. 2 shows for the volume-exclusion–only simulations, as a function of x_{Li}, (a) the calculated self- and collective-correlation factors, f and f_I, (b) average tetrahedral and octahedral site occupations, n_{tet} and n_{oct}, (c) tracer and "jump" diffusion coefficients, D^* and D_J, (d) and a reduced ionic conductivity, σ' (Eqn. 13).

In the single particle limit, $x_{Li} \to 0$, both correlation factors equal 1. There are no blocking effects, and particles follow a random walk. With increasing concentration of mobile ions, however, single particle diffusion increasingly deviates from random walk behaviour. The tracer correlation factor, f, decreases from $f = 1$ in the single particle limit $f = 0.25$ in the single vacancy limit $x_{Li} \to 9$, showing approximately linear dependence on

x_{Li}.[62]

The magnitude of the tracer correlation effect can be compared across different lattice geometries by considering f in the limit of a single vacancy, f_{v}. Table I presents values previously calculated for simple 3D lattices,[63] for a 1D chain,[14], and our result for the garnet lattice. The garnet lattice value of $f_v = 0.25$ is smaller than for all of the other 3D lattices listed, and is a factor of two less than the next lowest (the diamond lattice). This indicates that the garnet lattice exhibits particularly strong site blocking effects. This can be understood as a consequence of the garnet lattice geometry. For a general set of 3D lattices, as the number of nearest neighbours of each lattice site, z, decreases, f_v also decreases, and correlation effects become more significant. The garnet lattice has both 4-coordinate (tetrahedral) and 2-coordinate (octahedral) sites, and long ranged diffusion follows an alternating tet→oct→tet→oct sequence. The calculated value of $f_v = 0.25$ is halfway between the values for the 4-coordinate diamond lattice ($f_v = 0.5$) and for a 1-D chain, where every site is 2-coordinate ($f_v = 0$).[14] This suggests that the extreme low value of f_v for the garnet lattice is a consequence of the low coordination of the lattice sites, in particular the local 1D coordination at the octahedral sites, which act as bottlenecks for long-ranged diffusion.

Lattice	z	f_v
Face centered cubic[63]	12	0.78146
Body centred cubic[63]	8	0.72722
Simple cubic[63]	6	0.65311
Diamond[63]	4	0.5
Garnet [This work]	4+2	0.25
1D chain[14]	2	0.0

TABLE I. Vacancy correlation factors for some common crystal lattices. z is the number of nearest neighbours for each site in the lattice.

For any non-interacting system, the hops made by *different* particles are unocorrelated, and $f_I = 1$ for all x_{Li}, hance $H_{\mathrm{R}} = f$. There are also no correlations between site occupations, and the mobile particles are randomly distributed over the available octahedral and tetrahedral sites, with a 2:1 population ratio that reflects the underlying lattice geometry.[64]

We also calculate three explicit measures of ionic transport in this system.[65] Fig. 2(c) shows the tracer diffusion coefficient, D^* (Eqn. 4) and the "jump diffusion coefficient", D_{J},[5] calculated as

$$D_{\mathrm{J}} = \frac{\left|\sum_i R_i\right|^2}{6Nt}. \tag{12}$$

At a fixed temperature D_{J} is proportional to the mobility, and measures the ease with which the mobile particles collectively migrate. Both D^* and D_{J} decrease monotonically from $x_{\mathrm{Li}} = 0$ to $x_{\mathrm{Li}} = 9$ ($x = 0 \to 1$), as the number of vacancies available to accomodate hopping decreases.

For the non-interacting system there are no correlations between hops made by different particles, and the jump diffusion coefficient is proportional to $(1-x)$ (in the garnet lattice, $x = 1$ corresponds to $x_{\mathrm{Li}} = 9$).[5,59] The tracer diffusion coefficient, however, is affected by correlations between hops made by individual particles, and varies as $D^* \propto (1-x)f$.[66] The ionic conductivity of a system depends on both the charge-carrier concentration, and the ionic mobility, which is proportional to D_J. We consider the relative effect of carrier concentration on ionic conductivity by considering a reduced conductivity, σ',[67] given by

$$\sigma' = xD_{\mathrm{J}}. \tag{13}$$

For any non-interacting system, $\sigma' \propto x\,(1-x)$, giving a maximum at $x = 0.5$, corresponding to $x_{\mathrm{Li}} = 4.5$ for the garnet lattice (Fig. 2(d)).

B. Interacting Particles

The conceptual simplicity of the non-interacting system makes it a useful starting point for understanding the factors affecting ionic transport in different lattices. In real Li-garnet materials, however, interactions between lithium ions, or between lithium ions and the host lattice, can be significant. Lithium ions carry positive charge, and can be expected to experience mutual Coulomb repulsion. The different oxygen-coordination environments of the octahedral and tetrahedral sites can be expected to produce a preference for occupation by lithium at one site versus the other.[68] Within the lattice-gas Monte Carlo scheme, we consider these two factors by introducing, first, nearest-neighbour repulsion, and second, an octahedral versus tetrahedral site preference.

1. *Nearest-neighbour repulsion*

To examine the effect of Li–Li repulsion, we consider a simplified model with only nearest-neighbour repulsion. The energy of Li at each specific site now depends on the number of occupied neighbouring sites. Individual hop probabilities therefore now depend on whether they increase or decrease the total number of nearest-neighbour pairs. Fig. 3 presents results from simulations performed for $E_{\mathrm{nn}} = 0.0$–$3.0\,kT$. Repulsive nearest-neighbour interactions disfavour simultaneous occupation of adjacent pairs of sites, which promotes ordering of particles across alternating occupied–vacant–occupied–vacant sites. This ordering causes the single-particle correlation behaviour to deviate from that of the non-interacting system, and also introduces collective correlations between the mobile ions.[10] f and f_{I} both have their non-interacting values in the empty and fully-occupied lattice limits: $x \to 0$ and $x \to 1$. In a lattice with only one crystallographic site complete ordering would occur at half–site-occupancy,

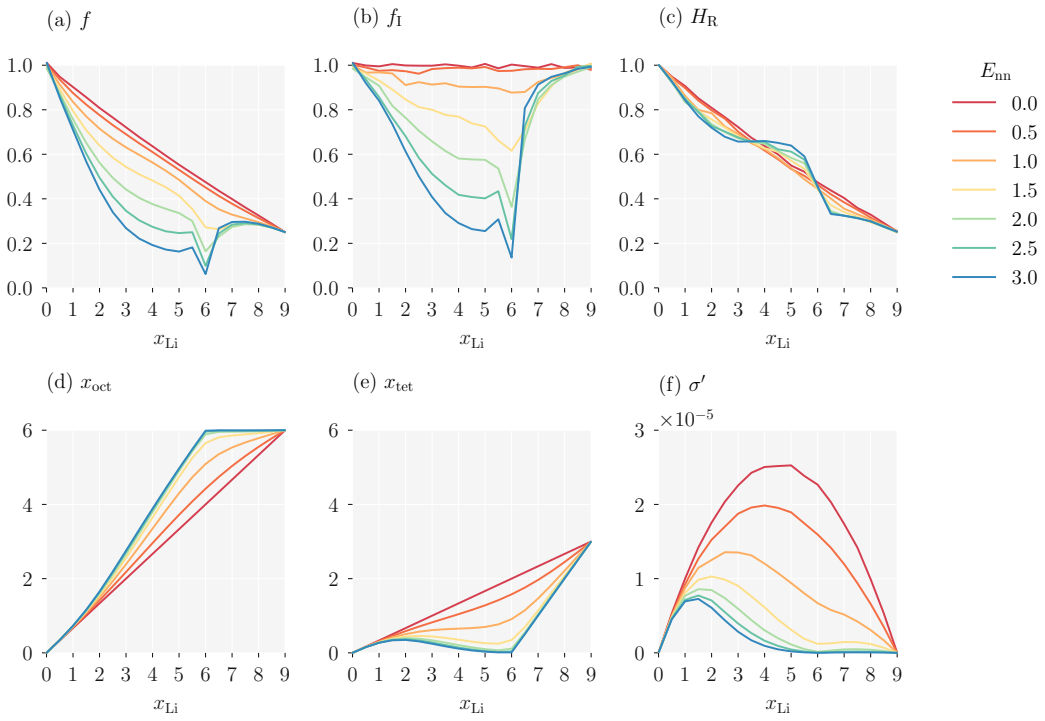

FIG. 3. The effect of nearest-neighbour repulsion between mobile particles on a garnet lattice: (a) single-particle correlation factor, f; (b) collective correlation factor, f_I; (c) Haven ratio, H_R; (d) average octahedra occupation, x_oct; (e) average tetrahedra occupation, x_tet; (f) reduced ionic conductivity, σ'. E_nn is in multiples of kT.

corresponding to $x_\mathrm{Li} = 4.5$ for the garnet lattice. f and f_I approximately follow this general trend (Fig. 3(a,b)), both decreasing at intermediate x_Li values as E_nn increases. Superimposed on this general trend, at moderate E_nn values, both correlation factors sharply decrease at $x_\mathrm{Li} = 6$, i.e. two-thirds occupancy. Because f and f_I do not change uniformly as E_nn is increased, the Haven ratio H_R develops a more structure. Perhaps most relevant to the lithium-stuffed garnets, above $x_\mathrm{Li} = 6$, the introduction of nearest-neighbour repulsion reduces H_R even further from the already low non-interacting value.

The garnet lattice contains octahedral and tetrahedral sites in a 2:1 ratio. In the non-interacting system, the average site occupancies follow this ratio across the full x_Li range (Fig. 2(b)). Introducing repulsive nearest-neighbour interactions increases the probability that octahedra are occupied relative to tetrahedra. Because octahedral sites are two-coordinate, versus the four-coordinate tetrahedral sites, preferentially occupying octahedral sites minimises the number of disfavoured nearest-neighbour interactions. This effect is strongest at two-thirds site occupation ($x_\mathrm{Li} = 6$) where a sufficiently large E_nn drives the system into a fully ordered arrangement with all the octahedral sites filled and all the tetrahedral sites empty. In this fully ordered system, correlation effects are maximised: a single ion hopping from octahedron to tetrahedron is blocked, and must return to its starting position. Diffusion becomes possible only for groups of particles undertaking highly correlated collective movement.[45] Both tracer diffusion and ionic conductivity are stringly reduced compared to their corresponding non-interacting system values, as seen in the changes in f and f_I. The collective correlations ($f_\mathrm{I} < 1$) are also visible in the reduced conductivity, σ', which decreases relative to the non-interacting system across the full x_Li range, with a notably strong decrease at $x_\mathrm{Li} = 6$.

2. *Asymmetric site-occupation energies*

In the non-interacting model, not only do mobile ions not interact with each other (excepting volume exclusion), but there are no relevant interactions between the mobile ions and the host lattice. Identifying a site as octahedral or tetrahedral only has relevance for defining the connectivity of the lattice graph. Mobile ions show an equal preference for octahedral and tetrahedral sites, with average occupations following a simple 2:1 ratio. This behaviour contrasts with experimental observations. Neutron data for lithium-garnets such as $Li_3Y_3Te_2O_{12}$ reveal that at $x_\mathrm{Li} = 3$ the lithium ions exclusively occupy the tetrahedral sites.[40,69] This suggests that at relatively low lithium concentrations, there is an energetic penalty for occupying octahedral rather than tetrahedral sites.[68] We model this difference in site-occupation energy by including a term $\Delta E_\mathrm{site} = E_\mathrm{oct} - E_\mathrm{tet}$. To investigate the effect of this ion–lattice interaction on ion dynamics and site occupations we performed a series of simulations for

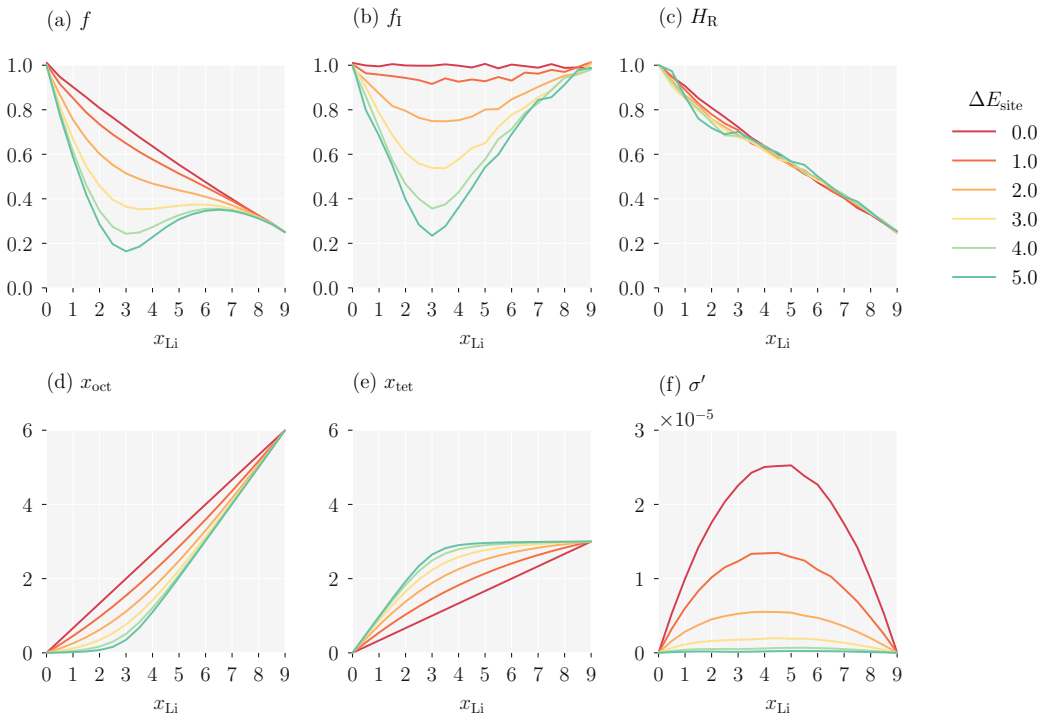

FIG. 4. The effect of unequal site occupation energies for mobile particles on a garnet lattice: (a) single-particle correlation factor, f; (b) collective correlation factor, f_I; (c) Haven ratio, H_R; (d) average octahedra occupation, x_{oct}; (e) average tetrahedra occupation, x_{tet}; (f) reduced ionic conductivity, σ'. ΔE_{site} is in multiples of kT.

otherwise non-interacting particles, with $\Delta E_{site} = 0$—$5kT$.

The effect of ion–lattice interactions qualitatively mirrors the effect of nearest-neighbour interactions (Fig. 4). Both single-particle and collective correlation factors are lower then their non-interacting values, average site occupancies deviate from those in the ideal system, and the reduced ionic conductivity decreases. Here, however, the strongest correlations emerge at $x_{Li} \approx 3$. As ΔE_{site} increases, tetrahedral sites are preferentially occupied with respect to octahedral sites, in contrast to the opposite behaviour observed when increasing nearest-neighbour repulsion. In the limit $T \to 0$ this again corresponds to a fully ordered arrangement of ions, now with all the tetrahedral sites filled and all the octahedral sites empty. The Haven ratio, H_R, shows less change compared to the non-interacting result, with only a small decrease for $x_{Li} < 3$.

3. *Combined site inequality and nearest-neighbour repulsion*

In real garnet electrolytes, lithium ions can be expected to interact with the host lattice, and also with each other. To explore the behaviour when both nearest-neighbour and site-occupation interactions exist we performed simulations to map the $\{x_{Li}, \Delta E_{site}, E_{nn}\}$ parameter space. The full data from these calculations is presented in Figs. A1–A4. With both interactions present, the ion dynamics and site occupation statistics are more complex, with specific details that depend on the precise values of both interaction terms. The general features, however, are illustrated by considering the subset for which $E_{nn} = \Delta E_{site}$ (Fig. 5). The correlation factors, f and f_I, both show sharp decreases at $x_{Li} = 3$ and $x_{Li} = 6$, in both cases corresponding to ordered arrangements of Li ions throughout the lattice. As in the previous single-interaction models, the ordering at $x_{Li} = 3$ corresponds to filled tetrahedra and empty octahedra (due to ΔE_{site}), and the the ordering at $x_{Li} = 6$ corresponds to filled octahedra and empty tetrahedra (due to E_{nn}). The average site occupation switches sharply from pure tetrahedral occupation to pure octahedral occupation in the range $x_{Li} = 3 \to 6$. The reduced ionic conductivity, σ', is depressed most strongly at lithium stoichiometries corresponding to the ordered arrangements of ions, again, mirroring the results for single interactions.

4. *Tuning lithium stoichiometry to maxmimise ionic conductivity*

One challenge regarding lithium garnet solid electrolytes is the identification of specific compositions with high ionic conductivities. For garnets with stoichiometries $Li_xA_3B_2O_{12}$, the lithium content can be continuously varied by choosing appropriate A and B cations, or by substituting Li^+ with small hypervalent cations such as Al^{3+} or Ga^{3+}. Different lithium stoichiometries

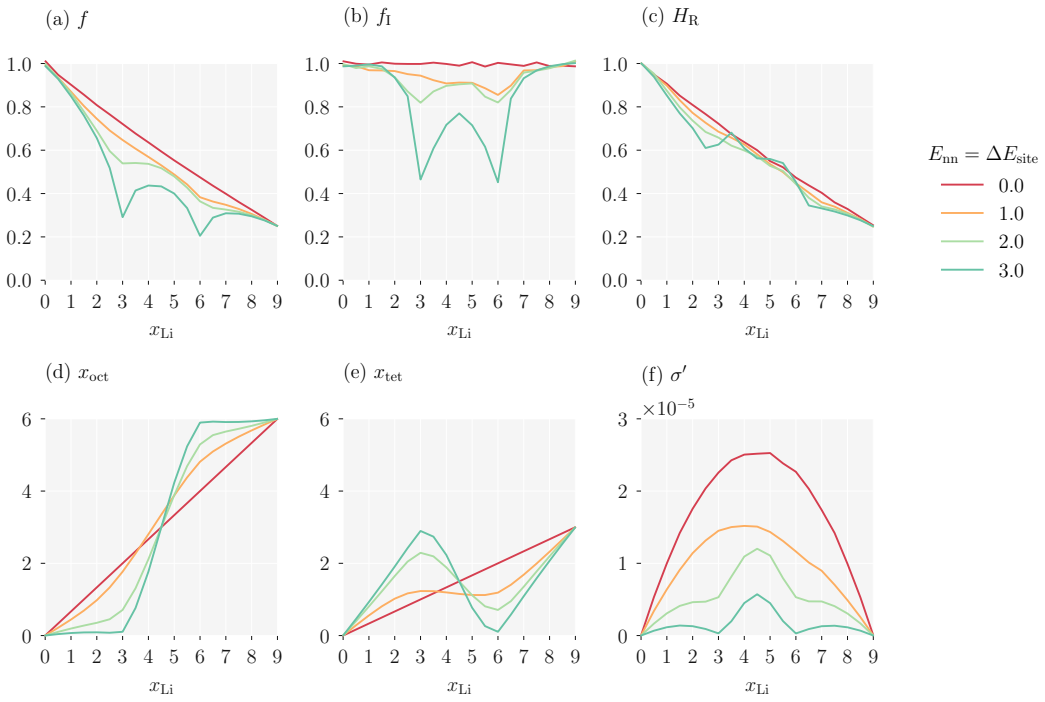

FIG. 5. The effect of combined nearest-neighbour repulsion and site-occupation energy differences on a garnet lattice, for $E_\mathrm{nn} = \Delta E_\mathrm{site}$: (a) single-particle correlation factor, f; (b) collective correlation factor, f_I; (c) Haven ratio, H_R; (d) average octahedra occupation, x_oct; (e) average tetrahedra occupation, x_tet; (f) reduced ionic conductivity, σ'. E_nn and ΔE_site are in multiples of kT.

can exhibit very different ionic conductivities. For example, at $x_\mathrm{Li} = 3$ (e.g. $Li_3Y_3Te_2O_{12}$) room temperature conductivities are typically too low to measure[1,31,40] while for $x_\mathrm{Li} \approx 6.5$ (e.g. $Li_{6.55}Ga_{0.15}La_3Zr_2O_{12}$) conductivities as high as $1.3\,\mathrm{S\,cm^{-1}}$ have been reported.[70,71] One conceptual approach to optimising the ionic conductivity, therefore, is to search for an "optimal" lithium stoichiometry.[36,50,72–78] A second approach is to consider how the ionic conductivity depends on the distribution of lithium ions over tetrahedral and octahedral sites.[30,36,76,79] This site distribution is itself a function of the lithium stoichiometry, modulated by the details of the interactions experienced by the lithium ions, as discussed above for the simple cases considered here.

For a non-interacting lattice gas, the ionic conductivity varies with the mole fraction of mobile particles, x, as

$$\sigma \propto x\,(1-x)\,. \tag{14}$$

The $(1-x)$ term is a "blocking factor" due to volume exclusion,[59] and the full dependence on carrier concentration is parabolic, as seen in the non-interacting system results presented above (Fig. 2(d)). For the lithium garnets this would correspond to a maximum ionic conductivity at $x_\mathrm{Li} = 4.5$. In real systems, the mobile ions are subject to additional interactions that introduce collective correlations, and the variation in ionic conductivity with mole fraction of mobile particles becomes

$$\sigma \propto x\,(1-x)\,f_\mathrm{I}. \tag{15}$$

Because f_I is itself a function of x, this gives non-trivial concentration dependence that cannot be described analytically. Furthermore, the concentration dependence of f_I is an emergent result of the specific interactions the lithium ions are subject to, which suggests that the mobile ion concentration that maximises the ionic conductivity in turn depends on the details of the lithium-ion interactions.

To explore this relationship in the model systems considered here, we identify the maximum reduced ionic conductivity as a function of lithium stoichiometry; $\arg\max \sigma'(x_\mathrm{Li})$; for each interaction parameter set $\{E_\mathrm{nn}, \Delta E_\mathrm{site}\}$. The resulting surface in parameter space is plotted in Fig. 6. As suggested by equation 15, the value of x_Li that maximises the ionic conductivity is strongly dependent on the interaction parameter values. $\arg\max \sigma'(x_\mathrm{Li}) = 4.5$ for the non-interacting system ($E_n n = 0$, $\Delta E_\mathrm{site} = 0.0$), but varies from < 1.5 to > 7.5 across the parameter range considered. Interestingly, the site-occupation energy difference has little effect in the limit of zero nearest-neighbour interactions. As E_nn increases, however, $\arg\max \sigma'(x_\mathrm{Li})$ deviates from the non-interacting value. At low values of ΔE_site, the optimal x_Li decreases. This can be associated with the strong suppression of collective ion transport close to $x_\mathrm{Li} = 6$ (cf. Fig. 3, Fig. A4). At high values of ΔE_site, however, the optimal x_Li increases, reaching a maximum value of ~ 7.5. Under these conditions, the preference to occupy

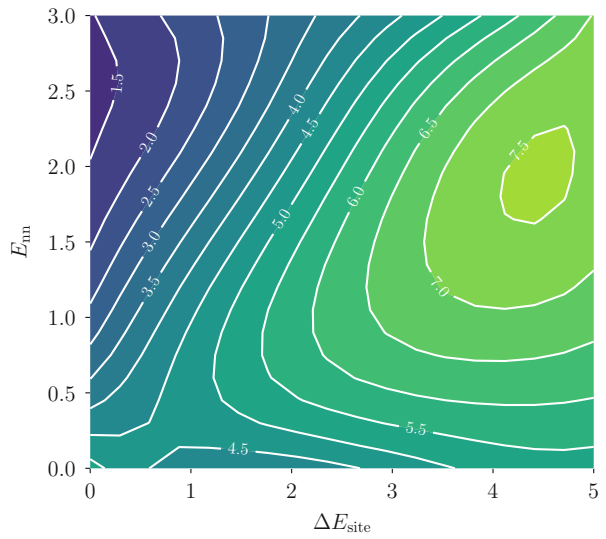

FIG. 6. Contour plot of the value of x_{Li} that maximises the reduced ionic conductivity, σ', as a function of nearest-neighbour interaction, E_{nn}, and on-site energy difference, ΔE_{site}: $f(E_{\mathrm{nn}}, \Delta E_{\mathrm{site}})$, $f = \arg\max \sigma'(x_{\mathrm{Li}})$.

tetrahedral sites dominates, and ion transport rates are strongly decreased close to $x_{\mathrm{Li}} = 3$ (cf. Fig. 4, Fig. A4).

IV. SUMMARY & DISCUSSION

Approximating ionic transport in solid electrolytes as particles undergoing random independent hops allows simple analytical relationships between microscopic hop rates and macroscopic transport coefficients to be derived (Eqns. 1 – 3). In real solid electrolytes these equations are exact only in the dilute limit. At moderate mobile ion concentrations, ion hops are not independent; Instead, they are correlated. The probability of a specific hop occurring depends on the instantaneous arrangement of other nearby ions. These hop correlations modify the quantitative relationships between hop rates and transport coefficients, with deviations from random walk behaviour expressed via the single-particle and collective correlation factors, f and f_{I}. Quantifying these correlation factors allows accurate converions between microscopic (hopping rates) and macroscopic (tracer diffusion coefficients and ionic conductivities) transport data. These factors also provide information about the ionic transport process: the single particle correlation factor quantifies the efficiency with which individual ions move through the electrolyte structure; the collective correlation factor provides an equivalent measure for the efficiency of mass or charge transport.

The simplest cause of correlation effects is volume exclusion, where ions occupying sites block the movement of a second ion. This "non-interacting" effect only causes single-particle correlations. The precise value of f depends on the concentration of mobile ions, and the geometry of the host lattice, which is a key difference between structural families of solid electrolytes. Including explicit interactions between the mobile ions, or between these ions and the lattice, superimposes additional single-particle correlation effect. These interactions also promote ordering of the mobile ions, which introduces collective correlations. In real solid electrolytes, therefore, the correlation behaviour depends on both lattice geometry and the nature of interactions acting on the mobile ions.

Here, we have explored this behaviour for the garnet lattice. This provides a model for the lithium diffusion network in lithium-garnet solid electrolytes. From a theoretical perspective, this lattice features intriguing topological properties. Previous theoretical and computational analyses of correlated ionic transport in crystalline lattices have considered only lattices where all sites are geometrically equivalent. The garnet lattice, however, contains both four-coordinate tetrahedral sites, and two-coordinate octahedral sites, arranged in an open 3D network of interconnected rings (Fig. 1).

To study correlation effects in the garnet lattice, we have performed kinetic lattice-gas Monte Carlo simulations.[61] These consider the host structure as an idealised lattice, and describe ion interactions through simple model Hamiltonians. While less "realistic" than performing explicit simulations of particular materials, using e.g. first-principles or classical molecular dynamics,[43,45] our approach benefits from being computationally cheaper, which allows a broad range of interaction models to be simulated, and from allowing changes in microscopic interactions to be transparently related to corresponding changes in transport behaviour.

We find that for the non-interacting (volume exclusion only) system, the single particle correlation effects due to the lattice geometry are more significant than for any previously studied 3D lattice (Table I). We propose that this is a consequence of the lattice containing two-coordinate octahedral sites, which act as bottlenecks to diffusion, and cause correlation effects intermediate between simple 3D and 1D lattices.

Explicit interactions acting on the mobile ions (e.g. nearest-neighbour repulsion and site-occupation energy differences) produce stronger single-particle correlation effects with a complex variation with x_{Li}. These explicit interactions also promote ordering at set mobile ion concentrations, which manifests as large collective correlation effects, with $f_{\mathrm{I}} \to 0$ as $T \to 0$.[10] The precise mobile-ion stoichiometry where ordering occurs depends on the lattice geometry and the explicit form of the interaction energy term. Ordering occurs for mobile-ion stoichiometries that are commensurate with the stoichiometry and symmetry of lattice sites, where ordering minimises the ion-interaction energy. In the cases considered here, nearest-neighbour repulsion promotes ordering at $x_{\mathrm{Li}} = 6$, with all octahedral sites occupied and all tetrahedral sites vacant; a site-occupation energy that

favours tetrahedral site occupation promotes ordering at $x_{\mathrm{Li}} = 3$, with all tetrahedral sites occupied and all octahedral sites vacant. The occupation of only tetrahedral sites at $x_{\mathrm{Li}} = 3$ is observed in experimental samples.[40] There are no experimental reports, however, of lithium ordering at $x_{\mathrm{Li}} = 6$. Interestingly, a different ordered phase has been predicted at $x_{\mathrm{Li}} = 6$ by Kozinsky *et al.*, using group theoretical analysis combined with density functional theory calculations.[80] In this phase, octahedra and tetrahedra are occupied in a 4.5:1.5 ratio, with lithium arranged to give a lower crystal symmetry than the ideal cubic garnet lattice (space group $P2_13$).

The ionic conductivity depends on the mobile ion concentration both directly, through the mole fractions of mobile ions and of vacant sites, and indirectly, through the collective correlation factor (Eqn. 15). Because the variation of f_{I} with x_{Li} depends on the form of the interaction energy, for models that go beyond volume-exclusion only there is no simple expression for the mobile-ion concentration that will maximise the ionic conductivity. The simulations presented here show that $\arg\max \sigma'(x_{\mathrm{Li}})$ is in fact very sensitive to the type and strength of mobile ion interactions, with the "optimal" lithium stoichiometry varying from $x_{\mathrm{Li}} = 1.5 - 7.5$ within the range of parameters considered. Even within the simplified models studied here, therefore, ionic transport on the garnet lattice exhibits correlation effects that are both more significant that predicted for simple 3D lattices, and that show a complex dependence on mobile ion stoichiometry.

The prediction that lithium garnet solid electrolytes exhibit strong correlation effects is consistent with the observation of highly cooperative diffusion processes in first-principles simulations.[42,43] Because the quantitative correlation behaviour is sensitive to the mobile-ion interactions, one question is how the interactions in real lithium garnet electrolytes might map to the effective interactions considered here. This sensitivity also raises the possibility of tuning ionic conductivities with isovalent substitution within the host lattice. As a simple example, selecting different lattice cations will modify the crystal lattice parameter, in turn changing both ΔE_{site} and E_{nn}. While f and f_{I} are sensitive to these parameters, their ratio $\frac{f}{f_{\mathrm{I}}} = H_{\mathrm{R}}$ is less so. The approximate Haven ratios presented here can therefore be used to improve the quantitative nature of conversions between tracer diffusion coefficients and ionic conductivities, via the modified Nernst-Einstein relation (Eqn. 6). For example, considering all the parameter sets considered here, the mean Haven ratio at $x_{\mathrm{Li}} = 7$ is 0.36 (Fig. 7).

Although f and f_{I} are much more sensitive to the interaction energy, it is clear that assuming that $f = f_{\mathrm{I}} = 1$ can introduce quantitative errors when converting between hop rates, and tracer diffusion coefficients or ionic conductivities. Here, we have discussed interaction energies scaled by the thermal energy, kT. In real systems, therefore, correlation factors will be temperature dependent. Correlation effects due to mobile ion interactions

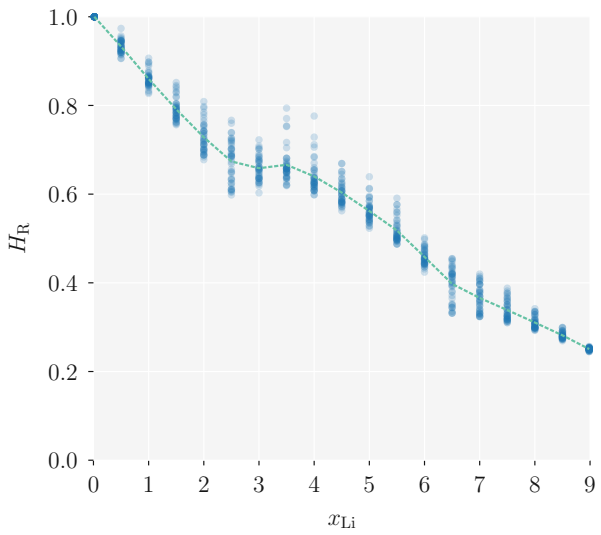

FIG. 7. Calculated Haven ratios for all interaction parameter sets considered, as a function of lithium stoichiometry, x_{Li}. The dashed line shows the mean values across these parameter sets.

therefore become less significant with increasing temperature. One consequence of this is that Arrhenius plots of tracer diffusion coefficient or ionic conductivities may not give straight lines, instead curving downwards as temperatures tend to zero, and correlation effects are enhanced. This behaviour is illustrated in Fig. 8, which shows an Arrhenius plot of relative ionic conductivities at $x_{\mathrm{Li}} = 6$, for non-interacting particles, using Eqn. 2, and for particles subject to nearest-neighbour repulsion. For the interacting case, f_{I} is interpolated from the simulation data described above, with the nearest-neighbour repulsion energy chosen as the Coulomb energy for two point charges occupying neighbouring sites, using a hopping activation energy of 0.3 eV and a typical garnet relative permittivity of $\epsilon_{\mathrm{r}} = 50$.[81] As the temperature decreases, correlation effects become stronger and f_{I} decreases, causing the Arrhenius plot to curve away from the straight line obtained for the non-interacting model. This additional temperature dependence means that empirical activation energies obtained by fitting to the data may deviate from the microscopic hopping activation energy. For the example considered here, the "observed" activation energy is 4.2 eV, compared to the hopping activation energy of 0.3 eV used to generate these data.

One of the limitations of this study is that it uses a fixed predetermined lattice geometry. The ordering predicted at $x_{\mathrm{Li}} = 3$ and $x_{\mathrm{Li}} = 6$ occurs at these lithium stoichiometries because these are commensurate with the lattice symmetry and site stoichiometry. In both cases, the ordered lithium configuration, with with either tetrahedral or octahedral sites fully occupied and the alternate site type fully vacant, preserves the lattice symmetry. In real materials lattice distortions are possible, and ordering of mobile ions can occur in concert with lattice

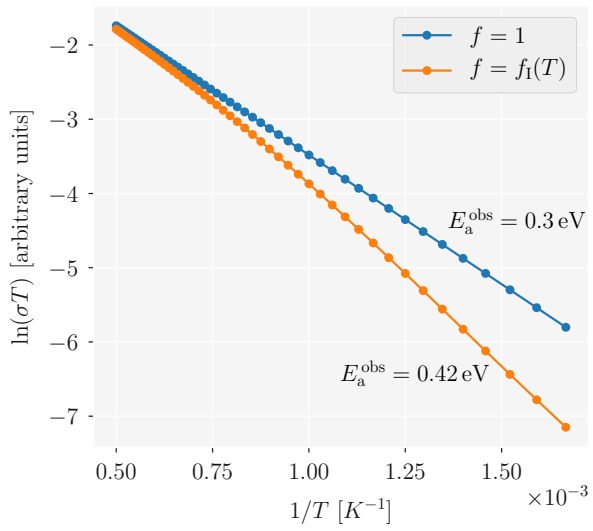

FIG. 8. Relative ionic conductivities calculated for non-interacting particles, using Eqn. 2, and for particles subject to nearest-neighbour repulsion, using Eqn. 5. For the interacting case, f_{I} is interpolated from the simulation data described above, with the nearest-neighbour repulsion obtained as the Coulomb energy for two point charges occupying neighbouring sites, using a typical garnet relative permittivity of $\epsilon_{\mathrm{r}} = 50$.[81] In each case an "observed" activation energy, $E_{\mathrm{a}}^{\mathrm{obs}}$, is derived by fitting a straight line to the low temperature $T \leq 1000\,\mathrm{K}$ data. Full details of this analysis are available in the supporting dataset.[82]

symmetry breaking. In the lithium garnets the prototypical example is the low-temperature tetragonal phase of $Li_7La3Zr2O_{12}$ (LLZO).[35,83] Although this material is cubic at high temperature ($T > 600\,\mathrm{K}$), at lower temperatures it undergoes a tetragonal distortion, associated with the lithium ions ordering to occupy all the octahedral sites and one third of the tetrahedral sites, and a decrease in ionic conductivity of two orders of magnitude. This is another example of ordering at low temperature, associated with low ionic conductivities as a consequence of enhanced correlation effects.[45] Again, the ordering occurs at a stoichiometry that is commensurate with the lattice symmetry. In the case of LLZO ordering is promoted at $x_{\mathrm{Li}} = 7$ because the tetragonal distortion lowers the crystal symmetry; in each lattice ring the six tetrahedral sites, that are equivalent by symmetry in the cubic lattice, become a set of (2+4) paired sites. Lithium ordering coupled to symmetry breaking has also been predicted at other lithium stoichiometries by Kozinsky *et al.*[80] Incorporating symmetry breaking effects into a lattice-gas Monte Carlo simulation scheme would require a more sophistocated approach than used here.

A second limitation of this study is the assumption that ion transport is effected by a sequence of discrete hops made by individual ions. This is not the case in *superionic* solid electrolytes,[84,85] where ions diffuse by highly concerted "liquid-like" processes. It is not known to what extent ion transport in solid lithium-ion electrolytes with high conductivities is effected by concerted rather than single-ion diffusion mechanisms.[86] In the case of the lithium garnets, data is limited. Meier *et al.* performed a first-principles metadynamics study of cubic LLZO, and their analysis predicted that concerted diffusion mechanisms do play a role in this particular system.[43] More recently, Chen *et al.* performed classical molecular dynamics simulations of LLZO, and found that in the cubic phase single-ion hopping is well described as a Poisson process,[78] which is characterstic of an independent hopping process.[87]. He *et al.* have performed first-principles nudge-elastic-band calculations that show that concerted diffusion processes can have low energetic barriers.[88]

The question of contributions from concerted diffusion processes is not only pertinent to high conductivity systems, but also to ordered phases with low ionic conductivities. Under strong ordering of mobile ions, the large correlation effects for single-particle hopping may sufficiently ion transport by this mechanism that alternate concerted mechanisms instead become the dominant means of ion transpoert.[45,87] In the context of developing a theoretical framework that can quantitatively connect microscopic diffusion processes in solid electrolytes to macroscopic transport coefficients, a general treatement of concerted diffusion mechanisms remains an intruiging problem.

V. SUPPLEMENTARY MATERIAL

Supplementary material for this study is available as a GitHub repository.[82] This repository contains (1) the complete data set used to support the findings of this study, (2) example scripts for running `lattice_mc` simulations on a garnet lattice and collating output data, and (3) a Jupyter notebook containing the code used to generate Figs. 2–A4. The `lattice_mc` code is available under the MIT license.[61]

VI. ACKNOWLEDGEMENTS

B. J. M. acknowledges support from the Royal Society (UF130329). B. J. M. would also like to thank M. Burbano and M. Salanne for stimulating discussions.

VII. APPENDIX

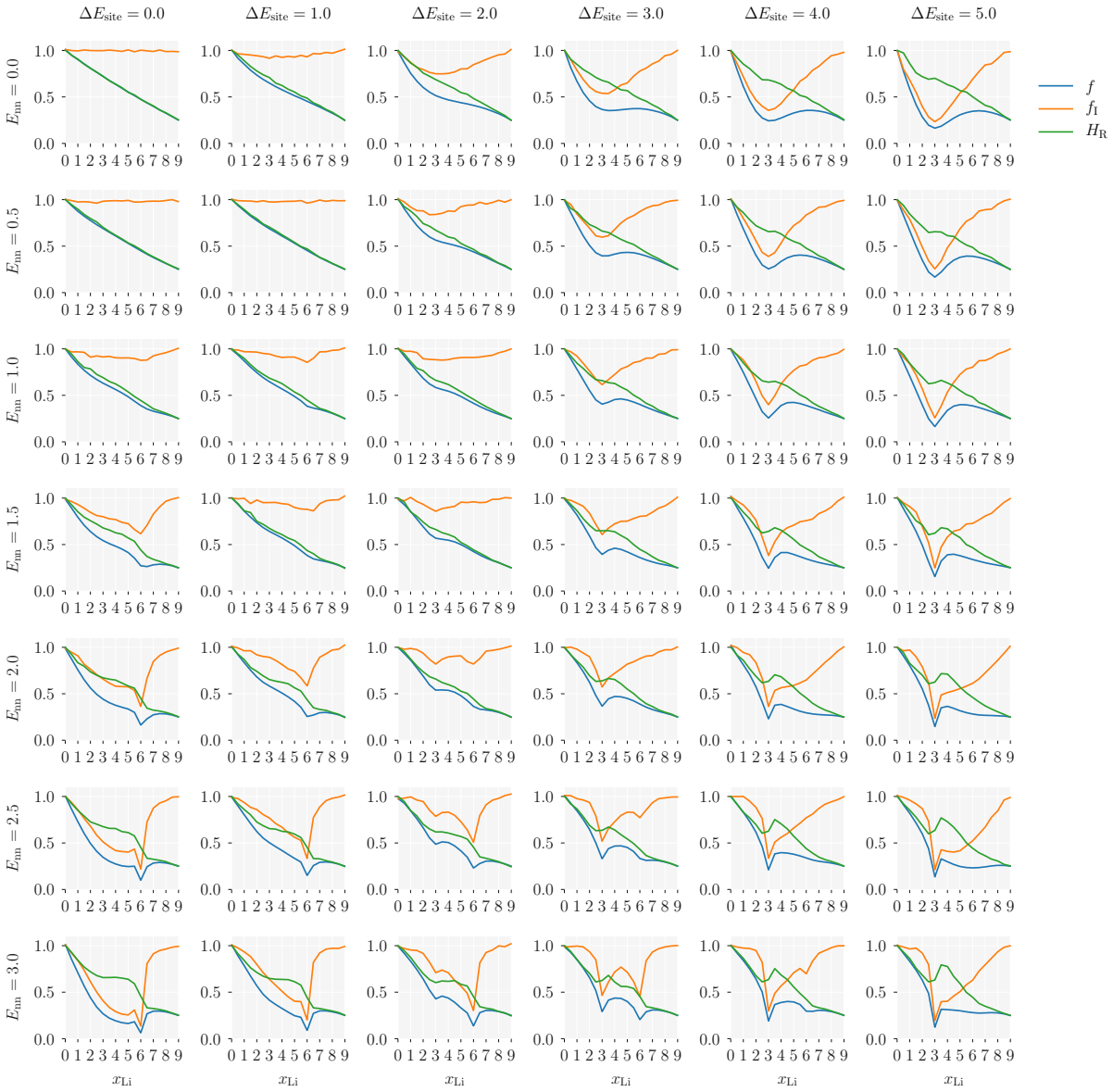

FIG. A1. Correlation factors for the garnet lattice as a function of mobile-ion stoichiometry, x_{Li}, nearest-neighbour repulsion, E_{nn}, and site-occupation energy difference, ΔE_{site}. Each subplot shows the single particle correlation factor, f, the collective correlation factor, f_{I}, and the Haven ratio, H_{R}.

[1] J. C. Bachman, S. Muy, A. Grimaud, H.-H. Chang, N. Pour, S. F. Lux, O. Paschos, F. Maglia, S. Lupart, P. Lamp, L. Giordano, and Y. Shao-Horn, Chem. Rev. **116**, 140 (2016).

[2] A. Manthiram, X. Yu, and S. Wang, Nat. Rev. Mater. **2**, 16103 (2017).

[3] J. B. Goodenough and P. Singh, J. Electrochem Soc. **162**, A2387 (2015).

[4] L. Malavasi, C. A. J. Fisher, and M. S. Islam, Chem. Soc. Rev. **39**, 4370 (2010).

[5] A. Van der Ven, J. Bhattacharya, and A. A. Belak, Acc. Chem. Res. **46**, 1216 (2013).

[6] Describing ionic transport as sequences of discrete hops breaks down for "super-ionic" solid electrolytes, with extremely mobile ions. The set of criteria for considering ionic transport to operate in a particle hopping regime are discussed by Catlow in C. R. A. Catlow, Sol. Stat. Ionics **8**, 89 (1983).

[7] The average hop rate per atom is the inverse of the mean residence time, $\widetilde{\nu} = 1/\widetilde{\tau}$. The contribution from each atom is a sum over individual hop rates, Γ_i, and is therefore related to the "total rate" of the kMC method via $\widetilde{\nu} = \langle Q \rangle / N$.[14].

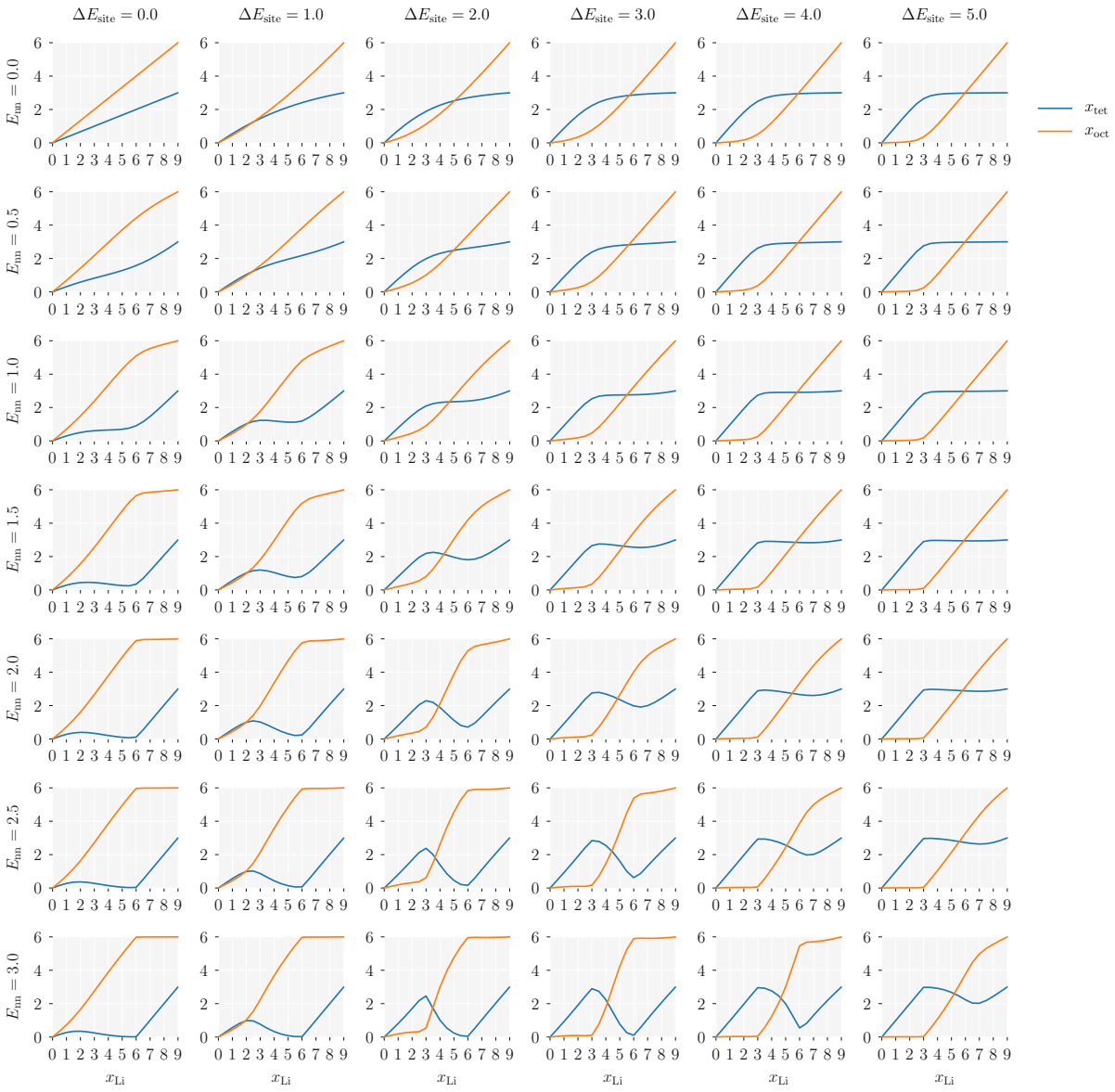

FIG. A2. Average site occupations for the garnet lattice as a function of mobile-ion stoichiometry, x_{Li}, nearest-neighbour repulsion, E_{nn}, and site-occupation energy difference, ΔE_{site}. Each subplot shows the time-averaged number of occupied tetrahedral, x_{tet}, and octahedral, x_{oct}, sites per formula unit.

[8] R. E. Howard and A. B. Lidiard, Rep Prog Phys. **27**, 161 (1964).
[9] A. M. Stoneham, ed., *Ionic Solids at High Temperatures* (World Scientific, 1989).
[10] G. E. Murch, Sol. Stat. Ionics **7**, 177 (1982).
[11] J. Bardeen and C. Herring, *Imperfections in Nearly Perfect Crystals* (John Wiley & Sons, Inc., 1952).
[12] K. Compaan and Y. Haven, Trans. Faraday Soc. **54**, 1498 (1958).
[13] A. R. Allnatt and A. B. Lidiard, *Atomic Transport in Solids* (Cambridge University Press, 2008).
[14] H. Mehrer (Springer, 2007).
[15] H. Sato and R. Kikuchi, J. Chem. Phys. **55**, 677 (1971).
[16] S. A. Akbar, J. Appl. Phys. **75**, 2851 (1994).
[17] M. Wilkening, W. Küchler, and P. Heitjans, Phys. Rev. Lett. **97**, 065901 (2006).
[18] B. Ruprecht, M. Wilkening, R. Uecker, and P. Heitjans, Phys. Chem. Chem. Phys. **14**, 11974 (2012).
[19] L. Enciso-Maldonado, M. S. Dyer, M. D. Jones, M. Li, J. L. Payne, M. J. Pitcher, M. K. Omir, J. B. Claridge, F. Blanc, and M. J. Rosseinsky, Chem. Mater. **27**, 2074 (2015).
[20] A. B. Santibáñez-Mendieta, C. Didier, K. K. Inglis, A. J. Corkett, M. J. Pitcher, M. Zanella, J. F. Shin, L. M. Daniels, A. Rakhmatullin, M. Li, M. S. Dyer, J. B. Claridge, F. Blanc, and M. J. Rosseinsky, Chem. Mater. **28**, 7833 (2016).
[21] H. Nozaki, M. Harada, S. Ohta, I. Watanabe, Y. Miyake, Y. Ikedo, N. H. Jalarvo, E. Mamontov, and J. Sugiyama,

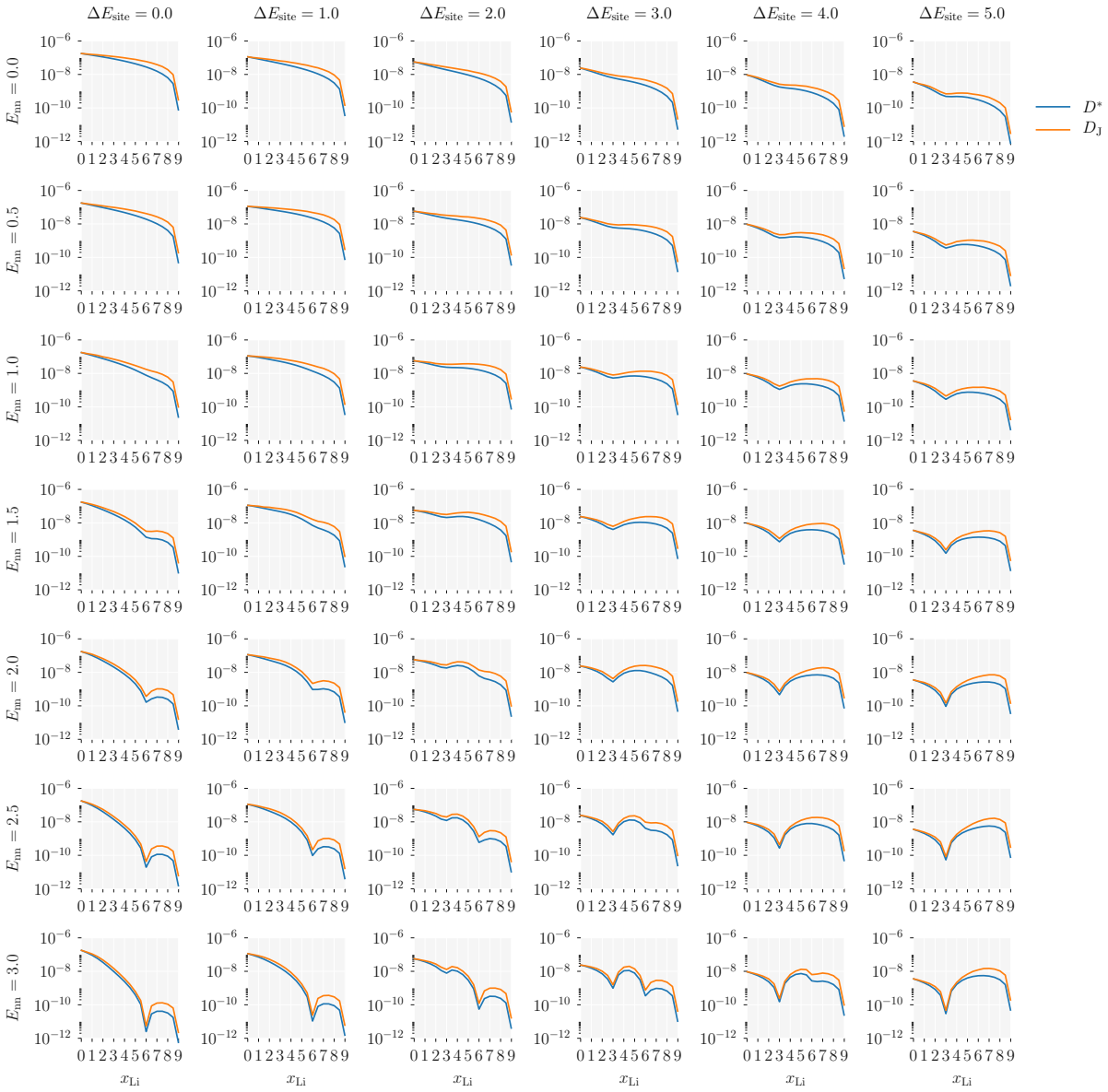

FIG. A3. Diffusion coefficients for the garnet lattice as a function of mobile-ion stoichiometry, x_{Li}, nearest-neighbour repulsion, E_{nn}, and site-occupation energy difference, ΔE_{site}. Each subplot shows the tracer diffusion coefficient, D^*, and the collective "jump" diffusion coefficient, D_J.

Sol. Stat. Ionics **262**, 585 (2014).

[22] M. Amores, T. E. Ashton, P. J. Baker, E. J. Cussen, and S. A. Corr, J. Mater. Chem. A **4**, 1729 (2016).

[23] R. D. Bayliss, S. N. Cook, S. Kotsantonis, R. J. Chater, and J. A. Kilner, Adv. Energy Mater. **4**, 1 (2014).

[24] W. G. Zeier, S. Zhou, B. Lopez-Bermudez, K. Page, and B. C. Melot, ACS Appl. Mater. Int. **6**, 10900 (2014).

[25] B. Lopez-Bermudez, W. G. Zeier, S. Zhou, A. J. Lehner, J. Hu, D. O. Scanlon, B. J. Morgan, and B. C. Melot, J. Mater. Chem. A **4**, 6972 (2016).

[26] A. Van der Ven, G. Ceder, M. Asta, and P. Tepesch, Phys. Rev. Lett. **64**, 184307 (2001).

[27] M. Mantina, Y. Wang, R. Arroyave, L. Q. Chen, Z. K. Liu, and C. Wolverton, Phys. Rev. Lett. **100**, 215901 (2008).

[28] B. J. Morgan and P. A. Madden, J. Phys-Condens. Matter **24**, 275303 (2012).

[29] R. J. Friauf, J. Appl Phys. **33**, 494 (1962).

[30] V. Thangadurai, H. Kaack, and W. Weppner, J. Am. Ceram. Soc. **86**, 437 (2003).

[31] V. Thangadurai, D. Pinzaru, S. Narayanan, and A. K. Baral, J. Phys. Chem. Lett. **6**, 292 (2015).

[32] R. Inada, S. Yasuda, M. Tojo, K. Tsuritani, T. Tojo, and Y. Sakurai, Front. Energy Res. **4**, 336 (2016).

[33] X. Han, Y. Gong, K. K. Fu, X. He, G. T. Hitz, J. Dai, A. Pearse, B. Liu, H. Wang, G. Rubloff, Y. Mo, V. Thangadurai, E. D. Wachsman, and L. Hu, Nat Mater. **16**, 572 (2016).

[34] S. Ramakumar, C. Deviannapoorani, L. Dhivya, L. S. Shankar, and R. Murugan, Prog. Mater. Sci. **88**, 325

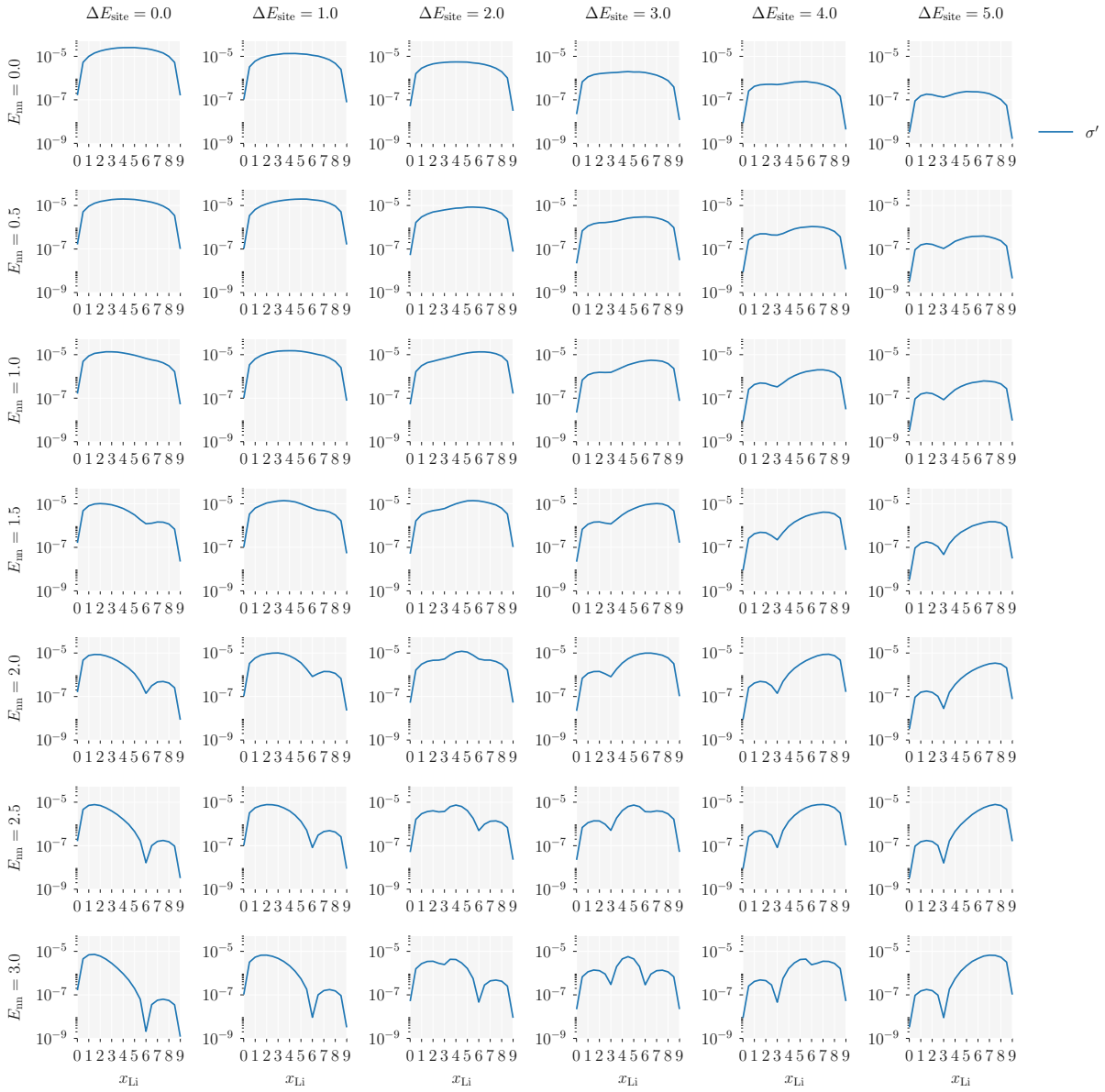

FIG. A4. Reduced ionic conductivity for the garnet lattice as a function of mobile-ion stoichiometry, x_{Li}, nearest-neighbour repulsion, E_{nn}, and site-occupation energy difference, ΔE_{site}. Each subplot shows the reduced ionic conductivity, σ' (Eqn. 13).

(2017).
[35] ICSD #422259J. Awaka, A. Takashima, K. Kataoka, N. Kijima, Y. Idemoto, and J. Akimoto, Chem. Lett. **40**, 60 (2011).
[36] M. P. O'Callaghan and E. J. Cussen, Chem. Comm. , 2048 (2007).
[37] M. P. O'Callaghan and E. J. Cussen, Sol. Stat. Sci **10**, 390 (2008).
[38] E. J. Cussen, J. Mater. Chem. **20**, 5167 (2010).
[39] Y. Wang, A. Huq, and W. Lai, Sol. Stat. Ionics **255**, 39 (2014).
[40] M. P. O'Callaghan, D. R. Lynham, E. J. Cussen, and G. Z. Chen, Chem. Mater. **18**, 4681 (2006).
[41] T. Thompson, A. Sharafi, and M. D. Johannes, Adv. Energy Mater. (2015).
[42] R. Jalem, Y. Yamamoto, H. Shiiba, M. Nakayama, H. Munakata, T. Kasuga, and K. Kanamura, Chem. Mater. **25**, 425 (2013).
[43] K. Meier, T. Laino, and A. Curioni, J. Phys. Chem. C (2014).
[44] M. Klenk and W. Lai, Phys. Chem. Chem. Phys. , 8758 (2015).
[45] M. Burbano, D. Carlier, F. Boucher, B. J. Morgan, and M. Salanne, Phys. Rev. Lett. **116**, 135901 (2016).
[46] M. J. Klenk and W. Lai, Sol. Stat. Ionics **289**, 143 (2016).
[47] M. Burbano, B. J. Morgan, and M. Salanne, "Li garnet md paper," In Preparation.
[48] A. Kuhn, S. Narayanan, L. Spencer, G. Goward, V. Thangadurai, and M. Wilkening, Phys. Rev. B **83**, 094302 (2011).

[49] A. Kuhn, V. Epp, G. Schmidt, S. Narayanan, V. Thangadurai, and M. Wilkening, J. Phys-Condens. Mat **24**, 035901 (2011).

[50] L. J. Miara, S. P. Ong, Y. Mo, W. D. Richards, Y. Park, J. M. Lee, H.-S. Lee, and G. Ceder, Chem. Mater. **25**, 3048 (2013).

[51] J. R. Rustad, arXiv (2016), related:H1H1zFMCzesJ.

[52] W. Gu, M. Ezbiri, R. P. Rao, M. Avdeev, and S. Adams, Sol. Stat. Ionics **274**, 100 (2015).

[53] S. Adams and P. P. Rao, J. Mater. Chem. **22**, 1426 (2012).

[54] A. Düvel, A. Kuhn, L. Robben, M. Wilkening, and P. Heitjans, J. Phys. Chem. C **116**, 15192 (2012).

[55] S. Narayanan, V. Epp, M. Wilkening, and V. Thangadurai, RSC Adv. **2**, 2553 (2012).

[56] A. Ramzy and V. Thangadurai, ACS Appl. Mater. Int. **2**, 385 (2010).

[57] Here we follow the convention where "non-interacting" does not preclude volume-exclusion, where two mobile particles are forbidden from simultaneously occupying a single lattice site.[59] This definition is equivalent to all allowed configurations of particles having equal energies.

[58] R. J. Trudeau, *Introduction to Graph Theory* (Dover Publications, Inc., 1993).

[59] R. Kutner, Phys. Lett. **81A**, 239 (1981).

[60] A. F. Voter, "Introduction to the kinetic monte carlo method," in *Radiation Effects in Solids*, edited by K. E. Sickafus, E. A. Kotomin, and B. P. Uberuaga (Springer Netherlands, Dordrecht, 2007) pp. 1–23.

[61] B. J. Morgan, J. Open Source Soft. **2** (2017), 10.21105/joss.00247.

[62] A linear least-squares fit to these data gives $R^2 = 0.9974$.

[63] K. Compaan and Y. Haven, Trans. Faraday Soc. **52**, 786 (1956).

[64] In the dilute limit an ion occupying a 4-coordinate tetrahedral site has four possible hops that allow it to escape. An ion occupying a 2-coordinate octahedral site has only two possible hops. For the non-interacting system, all hops are equally probably, hence the mean residence time for a tetrahedral site is half that of an octahedral site.

[65] Because the lattice-gas model used here considers hops as barrierless, where hopping probabilities only depend on energy differences between intial and final states, the effective transport coefficients calculated here cannot be directly compared to experimental values. Introducing fixed barrier heights for tet↔oct hops is equivalent to scaling the hopping prefactor ν', which preserves *relative* differences in the transport coefficients presented here. A more realistic model would need to account for the influence of local site occupations on individual hopping barriers, see e.g. Ref.[89], and would give quantitative deviations from the trends presented here.

[66] D_J is related to the ionic conductivity (via Eqns. 5 and 11) and also to the chemical diffusion coefficient, $\widetilde{D}$, via the thermodynamic factor, Θ, via $\widetilde{D} = D_\mathrm{J}\Theta$, where

$$\Theta = \frac{\partial\left(\frac{\mu}{kT}\right)}{\partial \ln x}. \tag{16}$$

.

[67] For a system with a single mobile species, the reduced conductivity is equal to the true ionic conductivity if $(VkT)/(q^2) = 1$.

[68] A preference for lithium to occupy tetrahderal rather than octahedral sites mirrors the results of Wang *et al.*, who have shown that for generic fcc and hcp lattices lithium similarly prefers to occupy tetrahedra. Y. Wang, W. D. Richards, S. P. Ong, L. J. Miara, J. C. Kim, Y. Mo, and G. Ceder, Nat. Mater. **14**, 1026 (2015).

[69] Several studies of "lithium-stuffed" garnets with $x_\mathrm{Li} \approx 7$ have also reported non-ideal distributions of lithium over tetrahedral and octahedral sites.[75] Here we focus on the lower concentration $x_\mathrm{Li} = 3$ data, where additional interactions, such as Li–Li repulsion, are expected to play less of a role.

[70] C. Bernuy-Lopez, W. Manalastas Jr., J.-M. López Del Amo, A. Aguadero, F. Aguesse, and J. A. Kilner, Chem. Mater. **26**, 3610 (2014).

[71] D. Rettenwander, C. A. Geiger, M. Tribus, P. Tropper, and G. Amthauer, Inorg. Chem. **53**, 6264 (2014).

[72] R. Murugan, V. Thangadurai, and W. Weppner, J. Electrochem Soc. **155**, A90 (2008).

[73] R. Murugan, V. Thangadurai, and W. Weppner, Ionics **13**, 195 (2007).

[74] S. Ramakumar, N. Janani, and R. Murugan, Dalton Trans. **44**, 539 (2015).

[75] H. Xie, J. A. Alonso, Y. Li, M. T. Fernández-Diaz, and J. B. Goodenough, Chem. Mater. **23**, 3587 (2011).

[76] R. Murugan, W. Weppner, P. Schmid-Beurmann, and V. Thangadurai, Mater. Sci. Eng.: B **143**, 14 (2007).

[77] M. Xu, M. S. Park, J. M. Lee, T. Y. Kim, Y. S. Park, and E. Ma, Phys. Rev. B **85** (2012).

[78] C. Chen, Z. Lu, and F. Ciucci, Sci. Rep. **7**, 40769 (2017).

[79] Y. Chen, E. Rangasamy, C. Liang, and K. An, Chem. Mater. **27**, 5491 (2015).

[80] B. Kozinsky, S. A. Akhade, P. Hirel, A. Hashibon, C. Elsässer, P. Mehta, A. Logéat, and U. Eisele, Phys. Rev. Lett. **116**, 055901 (2016).

[81] D. Rettenwander, A. Welzl, L. Cheng, J. Fleig, M. Musso, E. Suard, M. M. Doeff, G. J. Redhammer, and G. Amthauer, Inorg. Chem. **54**, 10440 (2015).

[82] B. J. Morgan, "Lithium-garnet lattice-gas Monte Carlo dataset," `https://github.com/bjmorgan/garnet-lgmc-data` (2017).

[83] N. Bernstein, M. Johannes, and K. Hoang, Phys. Rev. B **109**, 205702 (2012).

[84] C. R. A. Catlow, Annual Review of Materials Science **16**, 517 (1986).

[85] S. Hull, Rep. Prog. Phys. **67**, 1233 (2004).

[86] The highly concerted diffusion mechanisms that characterise superionic electrolytes are also typically associated with significant correlation effects and Haven ratios that deviate from $H_\mathrm{R} = 1$.[85,90].

[87] B. J. Morgan and P. A. Madden, Phys. Rev. Lett. **112**, 145901 (2014).

[88] X. He, Y. Zhu, and Y. Mo, Nature Communications **8**, 1 (2017).

[89] A. Van Der Ven and G. Ceder, in *Handbook of Materials Modelling* (2010) pp. 1–28.

[90] M. Salanne, D. Marrocchelli, and G. W. Watson, J. Phys. Chem. C , 120718111510003 (2012).